Journal of Molecular Structure 1026 (2012) 127–132

Contents lists available at SciVerse ScienceDirect

Journal of Molecular Structure

journal homepage: www.elsevier.com/locate/molstruc

DFT and QTAIM study of the tetra-*tert*-butyltetraoxa[8]circulene regioisomers structure

Gleb V. Baryshnikov [a], Boris F. Minaev [a,*], Valentina A. Minaeva [a,b], Alina T. Baryshnikova [a], Michael Pittelkow [c]

[a] Bohdan Khmelnytsky National University, 18031 Cherkasy, Ukraine
[b] Theoretical Chemistry, School of Biotechnology, Royal Institute of Technology, SE-10691 Stockholm, Sweden
[c] Department of Chemistry, University of Copenhagen, Universitetsparken 5, DK-2100 Copenhagen Ø, Denmark

HIGHLIGHTS

- Tetra-*tert*-butyltetraoxa[8]circulene regioisomers were studied by DFT method.
- Electronic density distribution was calculated by the QTAIM method.
- The presence of stabilizing non-valence bonds is detected by X-ray experiment.
- The H···H contacts are dynamically unstable due to high ellipticity.
- The energy of the H···H and CH···O contacts was estimated by the Espinosa equation.

ARTICLE INFO

Article history:
Received 6 March 2012
Received in revised form 24 May 2012
Accepted 24 May 2012
Available online 31 May 2012

Keywords:
Tetraoxa[8]circulene
Density functional theory
Bader method
Hydrogen bond
Critical point
Binding energy

ABSTRACT

The recently synthesized tetra-*tert*-butyltetraoxa[8]circulene regioisomers characterized by unusual solution-state aggregation behavior are calculated at the density functional theory (DFT) level with the quantum theory of atoms in molecules (QTAIMs) approach to the electron density distribution analysis. The presence of stabilizing intramolecular hydrogen bonds and hydrogen–hydrogen interactions in the studied molecules is predicted and the energies of these interactions are estimated with QTAIM. Occurrence of the CH···O bonds is detected by the single-crystal X-ray analysis for two regioisomers, obtained in high purity.

1. Introduction

The symmetric tetraoxa[8]circulenes [1–7] attract the research interest as a promising electroluminescent material for organic light-emitting diodes (OLEDs) [8–11]. The first reliable structure description of the simplest symmetric tetraoxa[8]circulene (Fig. 1a) was proposed by Erdtman and Högberg in 1968 [1]. They found that the tetraoxa[8]circulenes are thermally stable oxygen-containing aromatic compounds with a planar central cyclooctatetraene ring. In subsequent papers [2–7] they continued the study of the tetraoxa[8]circulenes by different experimental methods. The first DFT studies of the structure, UV–visible and vibrational spectra of the symmetric tetraoxa[8]circulene series (Fig. 1a–g) were published in our recent paper [8]. In Ref. [9] the IR and Raman spectra of the symmetric tetraoxa[8]circulenes 1a and 1f were discussed for the first time.

The present paper is devoted to comparative experimental and quantum-chemical study of the four possible tetra-*tert*-butyltetraoxa[8]circulene regioisomer structures (Fig. 2), which were previously obtained by mono-*tert*-butyl-1,4-benzoquinone tetramerization procedure [10].

Regioisomeric [10] mixture of tetra-*tert*-butyltetraoxa[8]circulenes (Fig. 2) was purified by standard column chromatography on silica gel using heptane as the mobile phase. Using that purification technique, we were able to separate the symmetrical tetra-*tert*-butyltetraoxa[8]circulene (**1**) from the other three possible regioisomers, presented in Fig. 2. Upon crystallization of the mixture of the remaining three regioisomers, it was possible to

* Corresponding author. Tel.: +380 472 376576; fax: +380 472 354463.
E-mail addresses: glebchem@rambler.ru (G.V. Baryshnikov), bfmin@rambler.ru (B.F. Minaev).

0022-2860/$ - see front matter © 2012 Elsevier B.V. All rights reserved.
http://dx.doi.org/10.1016/j.molstruc.2012.05.065

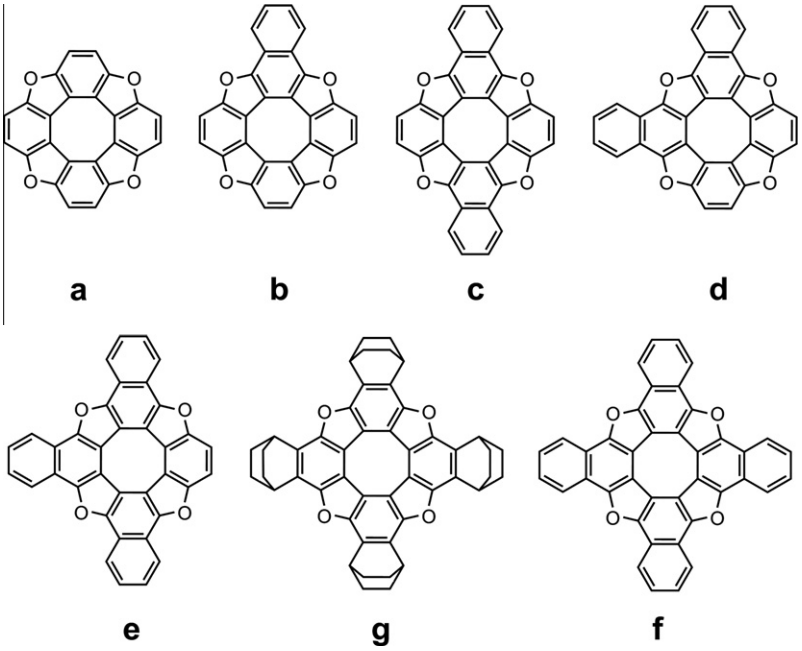

Fig. 1. The structure of symmetric tetraoxa[8]circulenes series.

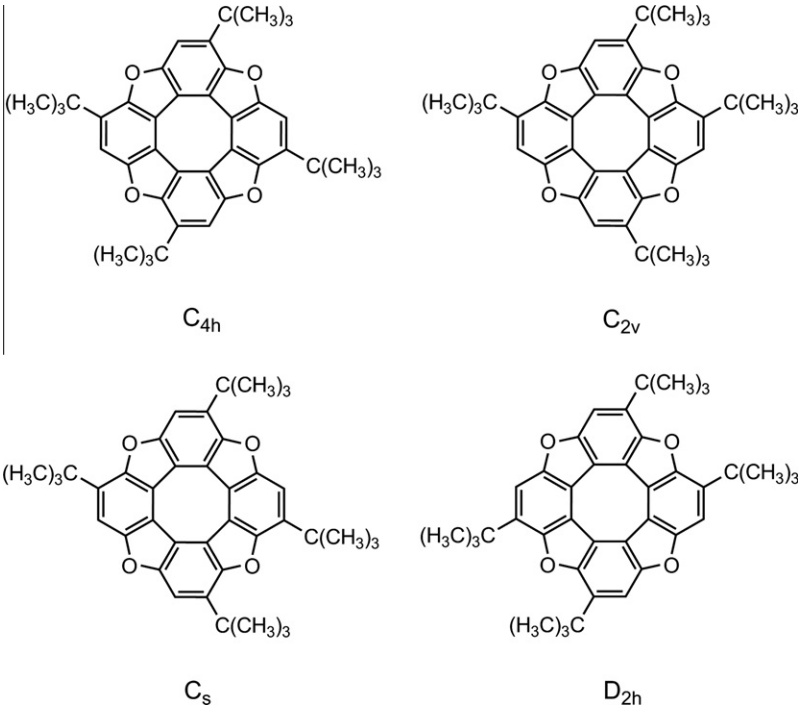

Fig. 2. The structure and symmetry point group of the tetra-*tert*-butyltetraoxa[8]circulene regioisomers.

crystallize in a high purity one of the twofold symmetrical isomers (Fig. 2; **2**). The regioisomers (**3**) and (**4**) in Fig. 2 were not separated from the mixture. They were characterized by NMR spectroscopy which data have approved the existence of both regioisomers (**3**) and (**4**) in the regioisomeric mixture.

It was found [10] that the tetra-*tert*-butyltetraoxa[8]circulenes aggregate in solution through a cooperative polymerization mechanism despite an evident functionalisation with bulky *tert*-butyl substituents. Such fictionalization usually suppress aggregation, which proceeds through a cooperative polymerization mechanism [10]. It is known that substitution with *tert*-butyl groups gives high solubility for a number of large aromatic molecules in non-polar solvents. The bulky *tert*-butyl substituents usually prevent π–π stacking interactions, which leads to the absence of aggregation.

Regioisomers (**1**) and (**2**) of tetra-*tert*-butyltetraoxa[8]circulene (Fig. 2) were isolated and characterized by single-crystal X-ray analysis (CCDC-822561) [10]. It was determined that the π–π stacking interactions are absent in the crystal packing of regioisomer (**1**) (Fig. 3), but are present for the compound (**2**) crystal packing (Fig. 3). This fact is due to the irregular arrangement of

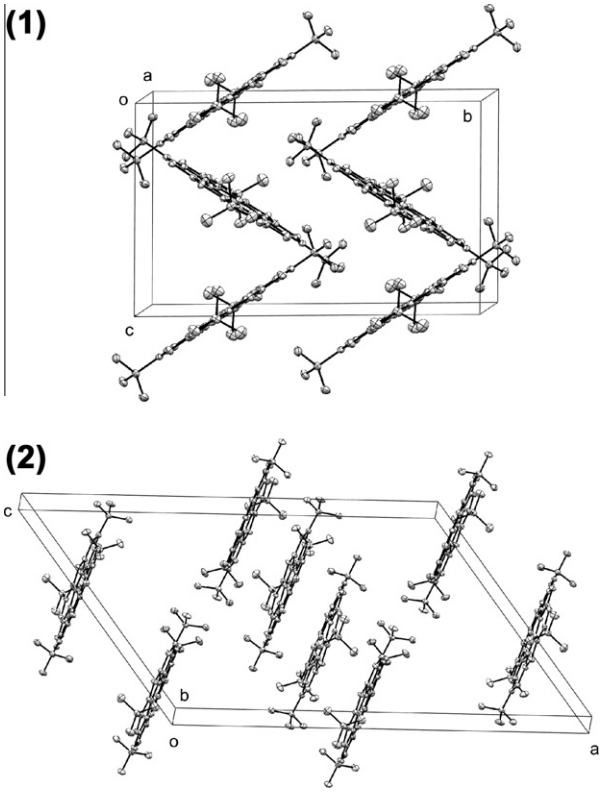

Fig. 3. The crystal packing of the tetra-*tert*-butyltetraoxa[8]circulene regioisomers (**1**) and (**2**), obtained from X-ray experiment by ORTEP visualization. (The similar figure is previously presented in Ref. [10], CCDC-822561).

tert-butyl substituents in the outer ring of the regioisomer (**2**). Thus we have assumed that the aggregation of the regioisomers (**1–4**) in solution is observed due to irregular arrangement of *tert*-butyl substituents in the formed regioisomers aggregates. This mechanism is similar to the "key-lock" principle. For example, the irregular arrangement of *tert*-butyl substituents in the compound (**2**) molecule provides the presence of the vacancies in the outer perimeter (determined by an absence of *tert*-butyl groups at the corresponding positions). These empty positions ("locks") in one molecule can contain the opposite *tert*-butyl substituents ("key") in other molecule. It should be clarified that conformational stability of the individual molecules determines the chemical composition of the regioisomeric mixture in a quantitative sence and explains the predominant chemical yield of compound (**1**) with the smaller yields of the impurities of isomers (**2–4**). Just the presence of the irregular regioisomers facilitates aggregation in solution and in solid state by the "key-lock" principle.

The results of our quantum-chemical calculations presented in this paper do illustrate a new aspect of the structure and intramolecular stabilization of the regioisomer molecules (**1–4**). In general one can say that the questions concerning tetraoxa[8]circulene structure represent a wide area of the upcoming studies in comparison with the well-studied problems related to annulenes [11], thiacirculenes and selenacirculenes [12].

2. Method of calculation

The equilibrium geometrical parameters of the molecules (**1–4**) presented in Fig. 4 were calculated by the DFT/B3LYP [13,14] method with the control of possible symmetry constrains using the double-valence-split Pople-type 6-31G(d) [15] basis set with the GAUSSIAN 03 package [16]. All vibrational mode frequencies were found to be real which indicates that a true minimum on hypersurface of the total energy was found.

For the optimized geometries of the molecules (**1–4**) a topological analysis of electron density distribution function $\rho(r)$ (therein r is the electron radius-vector) was performed by the Bader method named by "quantum theory of atoms in molecules" (QTAIMs) [17] with the AIMAll package [18]. This method strictly describes the criterion of existence of the interatomic binding interaction; namely: the presence of the bond critical point (CP) of the (3, −1) type and the presence of bond path between the interacting atoms is the necessary and sufficient condition of existence of the chemical bond (interatomic binding interaction) [19,20].

The position and type of electron density critical points for the studied structures was found. The number of CP for the studied molecules is a strictly subject to the Poincare-Hopf [17] relation for the limited stable molecular systems:

$$n - b + r - c = 1,$$

where n is a number of nuclei, or a number of (3, −3) critical points, b is a number of bonding lines (bonding interactions) or a number of (3, −1) critical points, r is a number of cycles (CP (3, +1)), c is a number of polyhedral cells (CP (3, +3)).

An important bond characteristic in the Bader theory terms is the value and sign of the electron density Laplacian $\nabla^2\rho$ in the bond critical point. The value of the Laplacian $\nabla^2\rho$ in the CP is a measure of electron density concentration in the interatomic space.

It is important that the $\rho(r)$ and $\nabla^2\rho$ values are experimentally verifiable by the precision X-ray diffraction analysis. Based on the $\rho(r)$ and $\nabla^2\rho$ values the local kinetic energy density $g(r)$ for the random molecular space point is approximately calculated by the Abramov gradient decomposition [21]:

$$g(r) = \frac{3}{10}(3\pi^2)^{\frac{2}{3}}\rho(r)^{\frac{5}{3}} + \frac{1}{72}\frac{[\nabla\rho(r)]^2}{\rho(r)} + \frac{1}{6}\nabla^2\rho(r),$$

For the bond critical point (3, −1) ($\nabla\rho = 0$ by definition) the $g(r)$, $v(r)$ and $h_e(r)$ values are experimentally calculated as the follows:

$$g(r) = \frac{3}{10}(3\pi^2)^{\frac{2}{3}}\rho(r)^{\frac{5}{3}} + \frac{1}{6}\nabla^2\rho(r),$$

$$v(r) = -\frac{3}{5}(3\pi^2)^{\frac{2}{3}}\rho(r)^{\frac{5}{3}} - \frac{1}{12}\nabla^2\rho(r),$$

$$h_e(r) = -\frac{3}{10}(3\pi^2)^{\frac{2}{3}}\rho(r)^{\frac{5}{3}} + \frac{1}{12}\nabla^2\rho(r).$$

The $h_e(r)$ value named as Cremer-Kraka electronic energy density [22] is equal to a sum of the $g(r)$ and $v(r)$ values: $h_e(r) = v(r) + g(r)$. Thus, the fundamental terms and concepts of the Bader theory find a quantitative confirmation from the precession X-ray diffraction analysis. This demonstrate a generality of the QTAIM formalism.

The (3, −1) bond critical point plays a key role in the molecular structure description, since the presence of CP (3, −1) is a necessary and sufficient condition for the binding interaction existence independently of the bond nature. As the critical points classification criterion the signs of the electron density Laplacian $\nabla^2\rho$ and electron energy density $h_e(r)$ in the critical point was proposed [22]:

(1) $\nabla^2\rho < 0, h_e(r) < 0$ – shared interactions (nonpolar and weakly polar covalent bonds).
(2) $\nabla^2\rho > 0, h_e(r) < 0$ – the intermediate type interactions (polar covalent bonds, strong hydrogen bonds, coordination bonds).
(3) $\nabla^2\rho > 0, h_e(r) > 0$ – the closed shell interactions (ionic bonds, weak hydrogen and Van der Waals bonds).

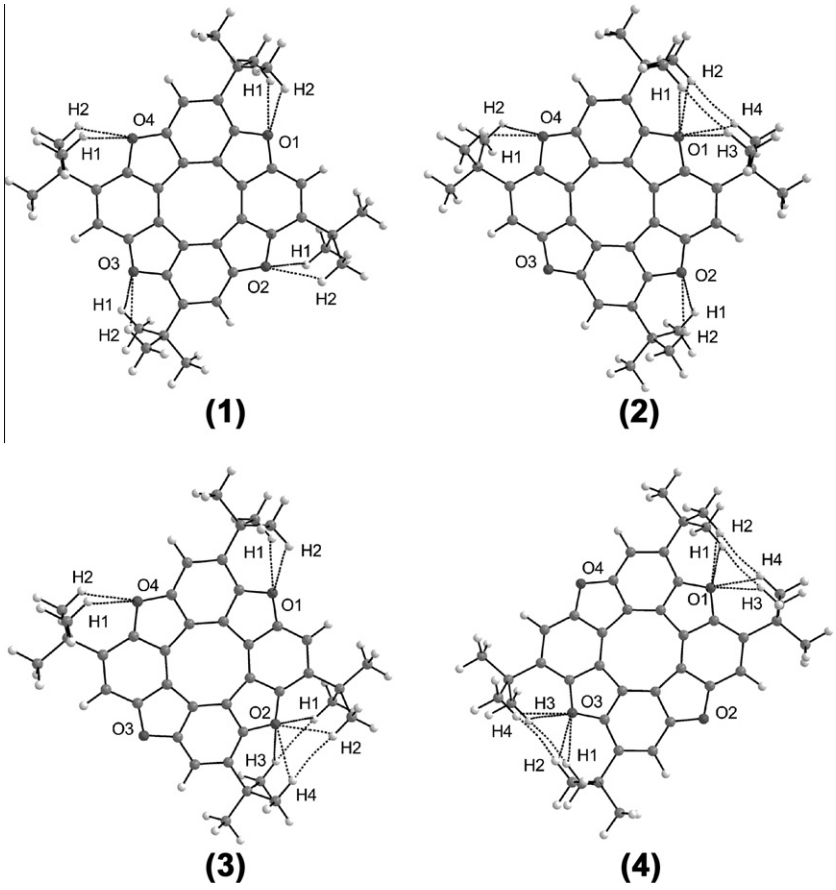

Fig. 4. The equilibrium molecular structure of the tetra-*tert*-butyltetraoxa[8]circulene regioisomers calculated by the DFT/B3LYP/6-31G(d) method. Intermolecular bonds are indicated by dashed line. Numbers (**1**–**4**) correspond to the structures shown in Fig. 2.

It is very important that the electron density analysis at the QTAIM level allows to identify very weak hydrogen bonds and Van der Waals contacts (e.g. CH···O, H···H, S···O, and C···N [23–26]) which are characterized by extremely low $\rho(r)$ values (at the critical point) measured experimentally by the high-precision X-ray diffraction analysis.

3. Results and discussion

Let us apply the QTAIM approach to analysis of the non-valent contacts in the tetra-*tert*-butyltetraoxa[8]circulene regioisomers in order to determine the conformation stability of the *tert*-butyl group position. In turn this will influence the "key-lock" aggregation mechanism. For the equilibrium molecular structure of the compounds (**1–4**), presented in Fig. 4, the number of electron critical points being subjected to the Poincare-Hopf relation is the following:

(**1**) $84 - 100 + 17 - 0 = 1$;
(**2** and **3**) $84 - 102 + 19 - 0 = 1$;
(**4**)$84 - 104 + 21 - 0 = 1$.

For the studied regioisomers the weak intramolecular CH···O and H···H interactions (Fig. 4) are predicted for the equilibrium molecular geometries on the ground of the calculated electron density distribution with DFT and QTAIM approaches. The analogous CH···O contacts are detected for the compounds (**1**) and (**2**) from the experimental data (Table 1) [10].

All predicted non-valent contacts are classified as the closed-shell interactions subjected to the third condition ($\nabla^2\rho > 0$, $h_e(r) > 0$). The calculated Laplacian values (Table 1) for the CH···O bonds are varied in the range 0.0380–0.0395 $e \cdot a_0^{-5}$, which coincides with the Koch-Popelier average range for a large number of the hydrogen bond examples (0.024–0.139 $e \cdot a_0^{-5}$) [27]. Obviously, the CH···O bonds are classified as the weak hydrogen bonds with the estimated bond energies in the range −2.29 to −2.45 kcal/mol. The energy of all detected bonds can be estimated by the Espinosa equation [28]:

$$E = \frac{1}{2}v(r)$$

where E is the energy of interatomic interaction (a.u.). Espinosa equation is valid for all types of hydrogen bonds, Van der Waals interactions and weak contacts such as H···H and CH···O interactions. The electron density $\rho(r)$ values (Table 1) in the CH···O bonds critical points are varied in the 0.0101–0.0108 $e \cdot a_0^{-3}$ range, which coincides with generalized Koch-Popelier range (0.002–0.035 $e \cdot a_0^{-3}$) [27].

The ratio of the curvature elements λ_1 and λ_3 qualitatively describes the type of the corresponding chemical bonds [17,29]. If $|\lambda_1/\lambda_3| > 1$, the sharing of the electron density in the interatomic space takes place, which corresponds to the covalent type of interaction. On the contrary, if $|\lambda_1/\lambda_3| < 1$, the electron density is concentrated in the near-nuclear space and this corresponds to the closed shells interactions (hydrogen bond, Van der Waals and ionic bonds). All predicted non-valent contacts are classified by this criteria as the closed-shell interactions, similarly to the third condition ($\nabla^2\rho > 0$, $h_e(r) > 0$). The ratio $|\lambda_1/\lambda_3|$ values vary in the 0.1707–0.1732 and

Table 1
Topological parameters of non-valence interactions in the compounds **1–4**.

Isomer	Bond	n [a]	d, Å	$\rho(r), e \cdot a_0^{-3}$	$v(r)$, a.u.	$h_e(r)$, a.u.	$\nabla^2\rho$, $e \cdot a_0^{-5}$	ε	E, kcal/mol
1	O(1)···H(1)	8	2.440 2.462[b]	0.0108	−0.0078	0.0010	0.0394	0.14	−2.45
2	O(1)···H(1)	4	2.440 2.253[b]	0.0107	−0.0078	0.0010	0.0394	0.14	−2.45
	O(2)···H(1)	4	2.464 2.447[b]	0.0102	−0.0074	0.0011	0.0382	0.20	−2.32
	H(1)···H(3)	2	2.417 2.629[b]	0.0040	−0.0016	0.0011	0.0151	1.60	−0.50
3	O(1)···H(1)	2	2.439	0.0108	−0.0078	0.0010	0.0395	0.14	−2.45
	O(4)···H(1)	2	2.444	0.0106	−0.0077	0.0010	0.0391	0.14	−2.42
	O(2)···H(1)	2	2.467	0.0101	−0.0073	0.0011	0.0382	0.20	−2.29
	O(2)···H(3)	2	2.465	0.0101	−0.0073	0.0011	0.0381	0.20	−2.29
	H(1)···H(3)	2	2.429	0.0040	−0.0016	0.0011	0.0148	2.60	−0.50
4	O(1)···H(1)	8	2.468	0.0101	−0.0073	0.0011	0.0380	0.20	−2.29
	H(1)···H(3)	4	2.445	0.0038	−0.0015	0.0011	0.0145	1.05	−0.47

[a] n is a number of equivalent bonds in a corresponding regioisomer.
[b] X-ray data (CCDC-822561) [10].

0.1838–0.1899 ranges for the CH···O and H···H contacts, respectively (Table 2).

An important feature of the bonding interactions in terms of the AIM theory is also a delocalization index (DI) of electron density between the bonded atoms. The DI value for any bonding interaction indicates the number of electrons shared in the interatomic space [17]. The delocalization index of the electron density is obtained by virtue of the Fermi hole density integration. In this case the DI value can be directly interpreted as a value of the bond order [30]. Taking into account that the studied CH···O and H···H bonds are classified as a weak non-valent contact, the DI values are relatively low and are varied in the 0.0293–0.0330 and 0.0107–0.0113 ranges for the CH···O and H···H contacts, respectively (Table 2).

The equilibrium geometrical parameters of the regioisomers (**1–4**) are calculated in this work with the control of possible symmetry constrains (Fig. 2). Therefore, some CH···O and H···H bonds are equivalent and have the same electron density distribution parameters. The total stabilization energy of the non-valent contacts is estimated by Espinosa equation (accounting the n coefficient, Table 1) and is equal to 19.60, 20.08, 19.90 and 19.26 kcal/mol for the regioisomers (**1–4**), respectively. A small contribution to the total stabilization energy of the regioisomers (**1–4**) is due to the presence of the H···H contacts between neighboring methyl groups. These contacts are theoretically determined for the (**2–4**) compounds and their energy are estimated to be in the range 0.47–0.5 kcal/mol (Table 1). It is obvious that these contacts are non-stable and can be broken down upon small displacement of the hydrogen atoms (as the result of methyl group rocking, for example). The dynamic instability of the H···H contacts is confirmed by the high ellipticity (ε) values (Table 1). The ellipticity is calculated as (λ_1/λ_2-1) and was suggested by Bader et al. for the quantitative description of the electron density deviation from the cylindrical symmetry in the CP of the (3, −1) type [31]. In fact, the value of ε is a measure of the π-component of the bonding [31]. In addition, the value of ε characterizes the cycle susceptibility to opening. The contacts with high ellipticity are potentially unstable. In such cases there is a high probability of bifurcation catastrophe, i.e. fusion of bond and ring critical points (CP (3, −1) and (3 + 1), respectively), which leads to unstable degenerate CP occurrence ($\omega < 3$). Thus, the predicted H···H contacts are unstable, but can be experimentally determined at a very low temperature, i.e. at the condition of a low thermal motion of atoms.

Table 2
Curvature elements, their ratio and delocalization index values of non-valence interactions in the compounds (**1–4**).

Isomer	Bond	λ_1, a.u.	λ_2, a.u.	λ_3, a.u.	$\lvert\lambda_1/\lambda_3\rvert$	DI
1	O(1)···H(1)	−0.0101	−0.0089	0.0585	−0.1732	0.0330
2	O(1)···H(1)	−0.0095	−0.0079	0.0556	−0.1709	0.0330
	O(2)···H(1)	−0.0101	−0.0089	0.0584	−0.1732	0.0294
	H(1)···H(3)	−0.0037	−0.0014	0.0203	−0.1838	0.0113
3	O(1)···H(1)	−0.0102	−0.0089	0.0586	−0.1733	0.0330
	O(4)···H(1)	−0.0100	−0.0088	0.0579	−0.1730	0.0327
	O(2)···H(1)	−0.0095	−0.0079	0.0554	−0.1707	0.0293
	O(2)···H(3)	−0.0095	−0.0079	0.0556	−0.1708	0.0294
	H(1)···H(3)	−0.0036	−0.0011	0.0196	−0.1852	0.0110
4	O(1)···H(1)	−0.0094	−0.0078	0.0552	−0.1707	0.0293
	H(1)···H(3)	−0.0035	−0.0003	0.0183	−0.1899	0.0107

If we neglect the H···H bonds energy, the total stabilization energy by virtue of the CH···O bonds (kcal/mol) for the regioisomer (**1–4**) molecules (**1**(19.6) > **2**(19.08) > **3**(18.9) > **4**(18.32)) is proportional to the relative total energy (kcal/mol) of regioisomers (**1**(0) > **2**(+0.77) > **3**(+0.78) > **4**(+1.33)). The lowest relative energy of the regioisomer (**1**) explains the predominant chemical yield of this compound upon the mono-*tert*-butyl-1,4-benzoquinone tetramerization reaction, which is accompanied with the smaller yields of the impurities of isomers (**2–4**), since their energies are close to the compound (**1**) energy value.

Further manifestations of the non-valent interactions in the studied tetra-*tert*-butyltetraoxa[8]circulene regioisomers will be investigated by vibrational IR and Raman spectra calculations and the luminescence spectra analysis with spin-orbit coupling and vibronic coupling accounts by the methods, described in the Refs. [8,9,32]. Preliminary results indicate the small frequency shifts and intensity changes for low-frequency vibrations of the *tert*-butyl groups.

4. Conclusions

The quantum-chemical study of the tetra-*tert*-butyltetraoxa[8]circulene regioisomers molecular structure by the DFT and QTAIM methods allows us to calculate the equilibrium conformations of studied molecules and to analyze the topological parameters of the electron density distribution. The presence of weak stabilizing hydrogen bonds and hydrogen–hydrogen interactions is assumed on the ground of the non-valent bond critical points analysis. The presence of the CH···O bonds is also detected by the experimental X-ray diffraction data for the two studied regiosomer

(**1** and **2**) molecules. For other two regiosomer molecules (**3** and **4**) the presence of the stabilizing CH···O and H···H contacts is theoretically predict for the first time, since they have not been extracted from the reactive mixture [10]. We also found, that the theoretically predicted H···H contacts can be experimentally detected at a low temperature (at the liquid helium temperature, for example), when atomic displacements are minimized. It is found, that the total stabilization energy due to the CH···O bonds presence determines the relative stability of the tetra-*tert*-butyltetraoxa[8]circulene regioisomers, which correlates with the total energy calculated with the B3LYP/6-31G(d) approach. The total stabilization energy of the non-valent contacts in the stable regioisomer molecular conformations is estimated by the Espinosa equation to be equal to 19 kcal/mol, approximately.

References

[1] H. Erdtman, H.E. Hogberg, Chem. Commun. (1968) 773.
[2] H. Erdtman, H.E. Hogberg, Tetrahedron Lett. 11 (1970) 3389.
[3] H.E. Hogberg, Acta Chem. Scand. 26 (1972) 309.
[4] H.E. Hogberg, Acta Chem. Scand. 26 (1972) 2752.
[5] H.E. Hogberg, Acta Chem. Scand. 27 (1973) 2559.
[6] H.E. Hogberg, Acta Chem. Scand. 27 (1973) 2591.
[7] J.-E. Berg, H. Erdtman, H.E. Hogberg, B. Karlsson, A.-M. Pilotti, A.-C. Soderholm, Tetrahedron Lett. 18 (1977) 1831.
[8] B.F. Minaev, G.V. Baryshnikov, V.A. Minaeva, Comput. Theor. Chem. 972 (2011) 68.
[9] V.A. Minaeva, B.F. Minaev, G.V. Baryshnikov, H. Agren, M. Pittelkow, Vib. Spectrosc. (2012), http://dx.doi.org/10.1016/j.vibspec.2012.02.005.
[10] T. Brock-Nannestad, C.B. Nielsen, M. Schau-Magnussen, P. Hammershøj, T.K. Reenberg, A.B. Petersen, D. Trpcevski, M. Pittelkow, Eur. J. Org. Chem. 2011 (2011) 6320.
[11] R. Salcedo, L.E. Sansores, A. Picazo, L. Sansyn, J. Mol. Struct.: Theochem. 678 (2004) 211.
[12] K. Yu Chernichenko, E.S. Balenkova, V.G. Nenajdenko, Mendeleev Commun. 18 (2008) 171.
[13] A.D. Becke, J. Chem. Phys. 7 (1993) 5648.
[14] C. Lee, W. Yang, R.G. Parr, Phys. Rev. B 37 (1988) 785.
[15] M.M. Francl, W.J. Petro, W.J. Hehre, J.S. Binkley, M.S. Gordon, D.J. DeFrees, J.A. Pople, J. Chem. Phys. 77 (1982) 3654.
[16] M. Frisch, G. Trucks, H. Schlegel, G. Scuseria, M. Robb, J. Cheeseman, J. Montgomery, J. Vreven, K. Kudin, J. Burant, J. Millam, S. Iyengar, J. Tomasi, V. Barone, B. Mennucci, M. Cossi, G. Scalmani, N. Rega, G. Petersson, H. Nakatsuji, M. Hada, M. Ehara, K. Toyota, Fukuda, J. Hasegawa, M. Ishida, T. Nakajima, Y. Honda, O. Kitao, H. Nakai, M. Klene, X. Li, R.J. Knox, H. Hratchian, J. Cross, V. Bakken, C. Adamo, J. Jaramillo, R. Gomperts, R. Stratmann, O. Yazyev, A. Austin, R. Cammi, C. Pomelli, J. Ochterski, P. Ayala, K. Morokuma, G. Voth, P. Salvador, J. Dannenberg, V. Zakrzewski, S. Dapprich, A. Daniels, M. Strain, O. Farkas, D. Malick, A. Rabuck, K. Raghavachari, J. Foresman, J. Ortiz, Q. Cui, A. Baboul, S. Clifford, J. Cioslowski, B. Stefanov, G. Liu, A. Liashenko, P. Piskorz, I. Komaromi, R. Martin, D. Fox, T. Keith, M. Al-Laham, C. Peng, A. Nanayakkara, M. Challacombe, P. Gill, B. Johnson, W. Chen, M. Wong, C. Gonzalez, J. Pople, Gaussian 03, revision C.02, Gaussian, Inc., Wallingford, CT, 2004.
[17] R.F.W. Bader, Atoms Inmolecules. A Quantum Theory, Clarendon Press, Oxford, 1990.
[18] T.A. Keith, AIMAll (version 10.07.25), www.aim.tkgristmill.com, 2010.
[19] R.F.W. Bader, J. Phys. Chem. A 102 (1998) 7314.
[20] R.F.W. Bader, Chem. Eur. J. 12 (2006) 2896.
[21] Yu A. Abramov, Acta Crystallogr. A 53 (1997) 264.
[22] D. Cremer, E. Kraka, Croat. Chem. Acta. 57 (1984) 1259.
[23] B.F. Minaev, G.V. Baryshnikov, V.A. Minaeva, Dyes Pigments 92 (2011) 531.
[24] G.V. Baryshnikov, B.F. Minaev, V.A. Minaeva, J. Struct. Chem. 52 (2011) 1051.
[25] I.V. Glukhov, K.A. Lyssenko, A.A. Korlyukov, M.Yu. Antipin, Rus. Chem. Bull. 54 (2005) 547.
[26] G.V. Baryshnikov, B.F. Minaeva, V.A. Minaeva, Z. Ning, Q. Zhang, Opt. Spectrosc. 112 (2012) 168.
[27] U. Koch, P.L.A. Popelier, J. Phys. Chem. 99 (1995) 9747.
[28] E. Espinosa, E. Molins, C. Lecomte, Chem. Phys. Lett. 285 (1998) 170.
[29] R.F.W. Bader, H. Essen, J. Chern. Phys. 80 (1984) 1943.
[30] C.L. Firme, O.A.C. Antunes, P.M. Esteves, Chem. Phys. Lett. 468 (2009) 129.
[31] R.F.W. Bader, T.S. Slee, D. Cremer, E. Kraka, J. Am. Chem. Soc. 105 (1983) 5061.
[32] B.F. Minaev, V.A. Minaeva, J. Fluoresc. 9 (1999) 221.